**Supplementary Figure Legends**

**Supplementary Fig. S1.** Secondary structure prediction of TERT motifs 3 and IFD. **(A)** Secondary structure prediction of TERT motif 1, 2, 3, A and B from representative species (*Homo sapiens, Oryzias latipes, Arabidopsis thaliana, Aspergilus fumigatus, Tetrahymena thermaphila, Euplotes aediculatus, Tribolium castaneum, Schizosaccharomyces pombe and Saccharomyces cerevisiae*). Predicted secondary structures (α-helices colored blue, β-sheets colored red, and random coil colored grey) and the crystal structure of *Tribolium* TERT (α-helices denoted by cylinders, β-sheets by arrows, and random coil by a black line) are shown below the amino acid sequence. The primary sequence of the entire RT domain (motif 1-E) was input in three online secondary structure prediction algorithms (YASPIN<http://zeus.cs.vu.nl/programs/yaspinwww>, PSI <http://bioinf.cs.ucl.ac.uk/psipred/psiform.html> and JPred <http://www.compbio.dundee.ac.uk/~www-jpred>), and the output were combined. The predicted structures of motif 1-B are shown. **(B)** Secondary structure prediction of TERT motif A, IFD and B from representative species.

**Supplementary Fig. S2.** Multiple sequence alignment from motif 2 to motif A of TERT, other RTs and RdRp. The TERT sequences includes additional species along with the representative species from **Fig. 1B**. The RT sequences are grouped as two monophyletic clades based on their evolutionary distance to TERT. The secondary structures (arrows: β-sheets, cylinders: α-helices) shown below the sequences are derived from the respective crystal structures of *Tribolium castaneum* TERT (3DU6), HIV1 RT (1HYS) and FMDV RdRp (1WNE). Motif 2 and A have identity/similarity set at 55% conservation, shaded black/grey with invariant residues are shaded in dark cyan and dark blue respectively. Red/light red shading indicates the motif 3 TERT identity/similarity. An analogous helix-turn-helix sequence within closely realted RTs has been previously identified as motif 2a. The identity/similarity for the residues in motifs 2 and A are derived from all sequences, while the linker/motif 3 identity/similarity is derived from each grouping. Consensus residues with 55% identity are shown below each group.

**Supplementary Fig. S3.** Additive effects of motif 3 mutations on telomerase activity and processivity. Mutant telomerase were reconstituted in RRL and assayed by using the conventional telomerase activity assay. The telomerase mutants that contain different combinations of the motif 3 mutations (del-643-649, V658A and the double mutation del-643-649/V658A) or the hTR template mutation (57C) were assayed as indicated. The relative activity and processivity of different mutants are shown below the gel. l.c.: loading control. The signal of each repeat added was normalized with dGTP incorporated and the signal of first repeat. $Log_{10}$[normalized intensity] was then plotted against repeat number. Processivity was derived using equation processivity=-ln2/(2.303k), where k is the slope of each line.

**Supplementary Fig. S4.** Multiple sequence alignment of the IFD region of TERT. IFD is divided into IFD-a, IFD-b, and IFD-c based on predicted secondary structure. The predicted secondary structures (as in Fig. S1) of *Homo sapiens* and *Tribolium castaneum* TERT are shown below the amino acid sequence. The secondary structures (arrows: β-sheets, cylinders: α-helices) shown below predicted structures are derived from the crystal structures of *Tribolium castaneum* TERT (3DU6). Shading of residues indicates 55% identity/similarity (black/grey). The four mutations in the yeast, *Saccharomyces cerevisiae* TERT (Est2) shown to decrease processivity are colored red within the yeast sequence. The mutation (790-VVIE-793-4A) in human TERT tested in this study is also colored red.

Supplementary Fig. S1

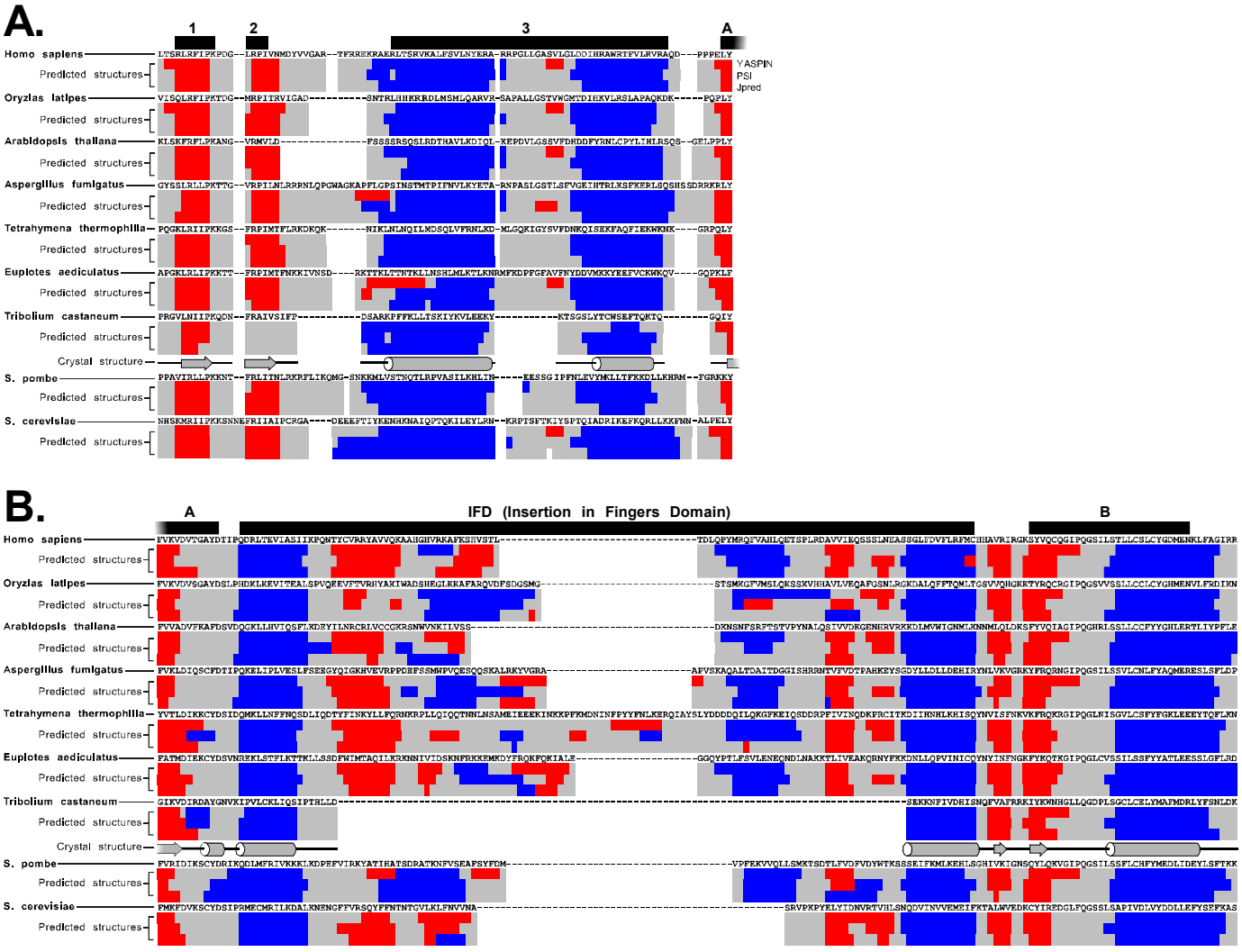

Supplementary Fig. S2

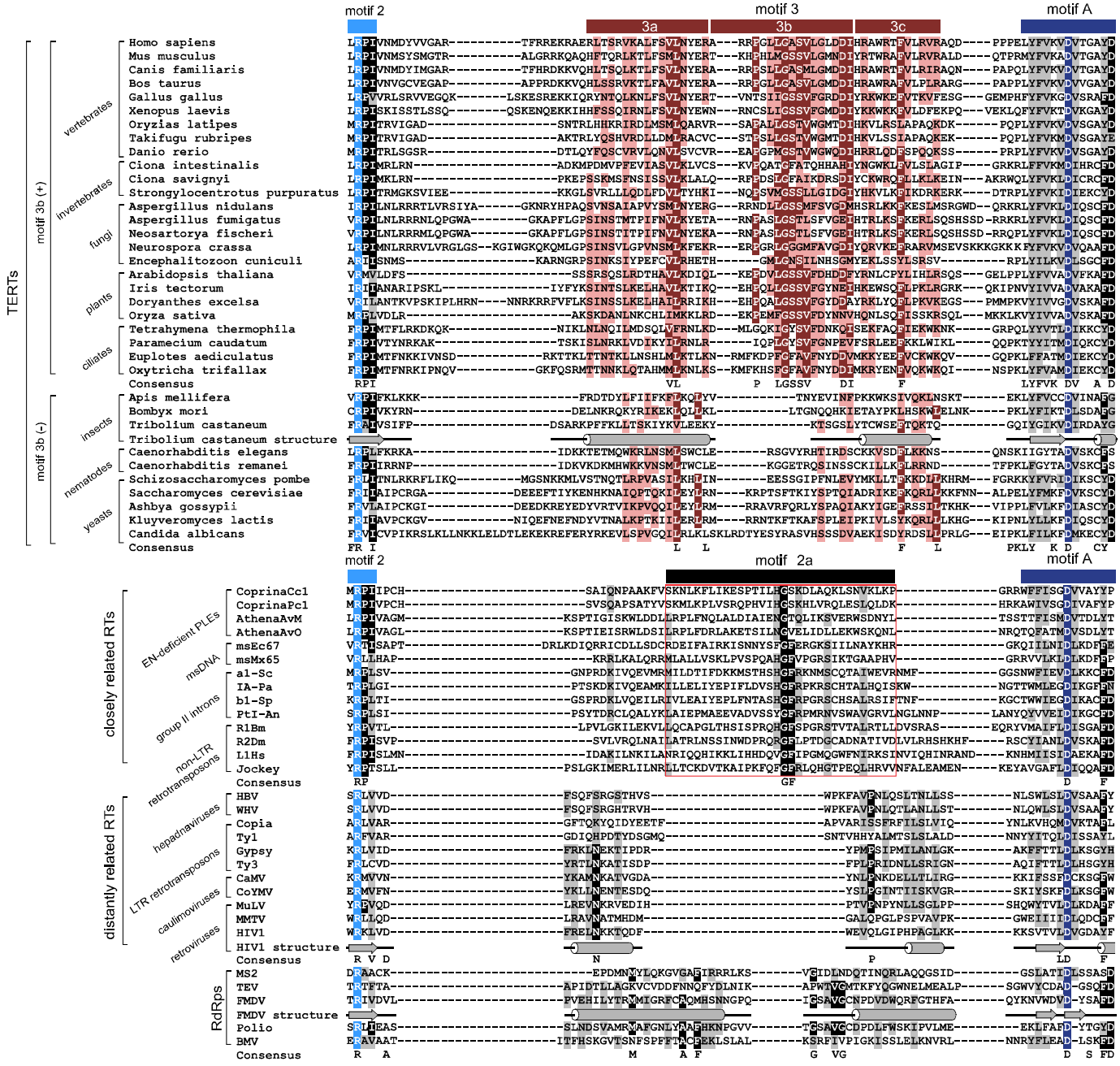

Supplementary Fig. S3

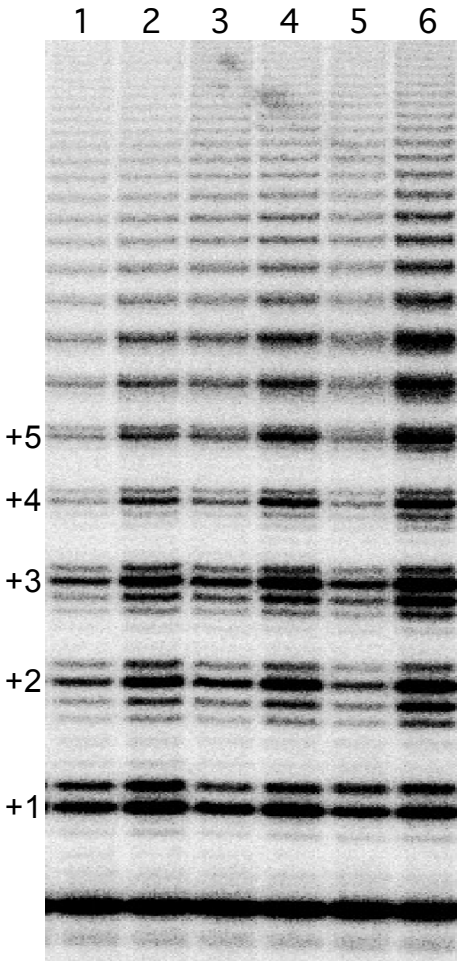


1. Wild-type
2. d643-649
3. V658A
4. d643-649/V658A (double)
5. hTR57C
6. d643-649/V658A/hTR57C (triple)

| | | | | | | |
|---|---|---|---|---|---|---|
| 100 | 174 | 131 | 219 | 127 | 281 | relative activity (%) |
| 100 | 91 | 113 | 98 | 108 | 113 | relative processivity (%) |

Supplementary Fig. S4